IEEE Photonics Journal
An IEEE Photonics Society Publication

Open Access

Stable Dissipative Soliton Generation From Yb-Doped Fiber Laser Modulated via Evanescent Field Interaction With Gold Nanorods

Volume 10, Number 5, September 2018

Shiyu Lu
Lin Du
Zhe Kang
Jie Li
Bin Huang
Guobao Jiang
Lili Miao
Guanshi Qin
Chujun Zhao
Shuangchun Wen

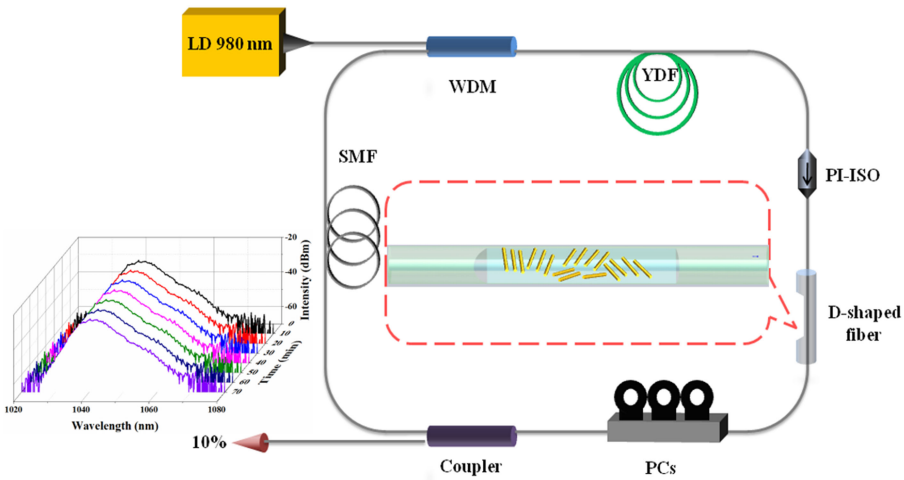

DOI: 10.1109/JPHOT.2018.2872405
1943-0655 © 2018 IEEE

Stable Dissipative Soliton Generation From Yb-Doped Fiber Laser Modulated via Evanescent Field Interaction With Gold Nanorods

Shiyu Lu,[1] Lin Du,[1] Zhe Kang,[2,3] Jie Li,[1] Bin Huang,[1] Guobao Jiang,[1] Lili Miao,[1] Guanshi Qin,[3] Chujun Zhao,[1] and Shuangchun Wen[1]

[1]Key Laboratory for Micro-/Nano-Optoelectronic Devices of Ministry of Education, School of Physics and Electronics, Hunan University, Changsha 410082, China
[2]Changchun Observatory, National Astronomical Observatories, CAS, Changchun 130117, China
[3]State Key Laboratory on Integrated Optoelectronics, College of Electronic Science & Engineering, Jilin University, Changchun 130012, China

DOI:10.1109/JPHOT.2018.2872405

Manuscript received August 10, 2018; revised September 13, 2018; accepted September 24, 2018. Date of publication September 27, 2018; date of current version October 11, 2018. This work was supported in part by the National Natural Science Foundation of China under Grants 61475102, 11574079, 61775056, and 61605219, in part by the Joint Equipment Pre-Research Foundation of the Ministry of Education of China under Grant 6141A02033404, and in part by the Natural Science Foundation of Hunan Province under Grant 2017JJ1013. Corresponding authors: Zhe Kang and Chujun Zhao (e-mail: kangz@cho.ac.cn; cjzhao@hnu.edu.cn).

Abstract: We demonstrated the dissipative soliton generation from a passively mode-locked ytterbium-doped fiber laser operating at 1041 nm by using evanescent field interaction with gold nanorods (GNR) saturable absorber (SA) experimentally. The GNRs, which have broadband longitudinal surface plasmon resonance absorption from ~800 to ~1500 nm, are synthesized by a seed-mediated growth method, and then composited with a D-shaped fiber to form the GNRs SA. The GNRs SA shows a modulation depth of 9.7% and low saturation intensity of 0.302 MW/cm^2. With the proposed GNRs SA, a dissipative soliton fiber laser was achieved with pulse duration 162.3 ps, repetition rate of 6.649 MHz at 1041 nm for a pump power of 220 mW. In addition, the signal-to-noise ratio can reach ~77 dB. The experimental result may make inroads for the nonlinear optical applications of the plasmonic nanomaterials.

Index Terms: Fiber lasers, mode-locked lasers, fiber non-linear optics, plasmonics.

1. Introduction

Ultrashort pulse Yb-doped fiber laser (YDFL) have attracted much interest in optical sensing, material processing, defense and military applications for their high stability, compact size, and efficient heat dissipation ability, which can make them practical alternatives to bulk laser systems [1]–[3]. Inspired by the requirements of the compact, stable, high pulse energy laser output, the fiber laser system operating in the all-normal-dispersion regime can provide an ideal solution with the help of the nonlinear saturable absorber (SA). With the evolution of the nonlinear optical materials, such as graphene [4]–[6], carbon nanotubes (CNTs) [7]–[9] and topological insulators (TIs)

[10]–[12], and the cavity optimization, the pulsed laser performance has been greatly improved. However, for the low-dimensional materials, the defect prone exfoliation and transfer processes inevitably lead to poor repeatability and reliability, and it has been challenging to tune the intrinsic nonlinear optical response in these systems. Therefore, it is necessary to find proper nonlinear optical material to improve the laser performance [13].

Gold nanorods (GNRs) are highly suitable plasmonic nanomaterials for the large third-order nonlinear response resulting from the surface plasmons resonance (SPR) characteristics [14]–[20]. Surface plasmons (SPs) refer to the electromagnetic oscillations generated by the excitation of a free electron and an electromagnetic field in a metal surface region under an external electromagnetic field [21], [22]. Because of the spherical symmetry of the gold nanoparticles, free electrons oscillate uniformly in all directions, so there is only one SPR band [23]. However, the GNRs have an irregular rod-like structure and their optical properties are not isotropic, so that there are two absorption peaks generated by transverse SPR absorption and longitudinal SPR absorption [24], [25]. By varying the aspect ratio of GNRs, it is possible to shift the linear and the nonlinear absorption behavior, which is the focus of theoretical and experimental research [26]. By controlling the aspect ratio of the GNRs, the longitudinal SPR absorption peaks can be located at 800–1500 nm, making it possible to act as a SA to achieve the desired mode-locked laser output [27]–[29]. When it comes to the fiber laser modulated by the SA, the method on how to integrate the nonlinear optical material into the fiber laser cavity is very important. The most popular method to integrate the nonlinear optical material is to sandwich the material between two fiber connectors via the transmissive way, since it offers the ease of integration into different fiber/waveguide systems. As for the GNRs, Z. Kang *et al*. have reported the mode-locked Yb-doped and Er-doped fiber laser with the transmissive type GNRs SA [24], [25]–[30]. However, the kind of SA will be liable to damage for the strong light illumination, and thus the laser performance was limited to relatively low pump and output power. In addition, the SA suffers from the limited interaction length between light and the nonlinear optical material, and the not compact configuration. Another integration method is to utilize the interaction between the evanescent field of waveguide and the nonlinear optical material, which can provide a good platform to alleviate the damage threshold and tune the linear or nonlinear interaction with an all-fiberized configuration [31]. X. D. Wang *et al*. have realized the mode-locked operation around the 1.5 μm spectral range based on the evanescent field interaction between microfiber and GNRs [28]. The microfiber can have strong evanescent field to interact with the GNRs, but the waveguide is not robust enough for the long-term operation, and the microfiber will be easy to introduce large loss and strong nonlinear for the small core size. Inspired by the requirements to realize a stable, compact and high-performance fiber laser, the mode-locked fiber laser via evanescent field interactions between light propagating along the D-shaped fiber and the GNRs to achieve mode-locking needs to be explored.

In this paper, we propose a simple and easy method to implement a passively mode-locked YDFL operating at 1041 nm by using GNRs SA. GNRs integrated onto a D-shaped fiber have been prepared to act as the SA compatible with an optical fiber cavity. By inserting the GNRs SA into the YDFL cavity pumped by a 980 nm laser diode, stable dissipative soliton pulses can be generated with an all-fiberized format. When a pump power reached 220 mW, the pulse width, output power and repetition rate of the 1041 nm mode-locked laser were 162.3 ps, 1.31 mW, and 6.649 MHz, respectively. In addition, the signal-to-noise ratio can reach $\sim$77 dB. The results obtained show that the integrated GNRs SA can be used to deliver stable dissipative soliton pulse with an all-fiberized YDFL.

2. The Preparation and Characterization of the Gold Nanorods

In the experiment, we used a seed-mediated growth method to synthesize GNRs based on previous reported preparation method [32]–[35]. Firstly, 5 mL of a 0.034 mol/L chloroauric acid ($HAuCl_4$) aqueous solution is uniformly mixed with 20 mL of 2 mol/L Hexadecyltrimethyl ammonium bromide (CTAB) solution in a beaker. The mixture solution was stirred at 60 °C for about 15 minutes. Then 1 mL of 0.0005 mol/L fresh sodium borohydride ($NaBH_4$) solution was injected into the above seed

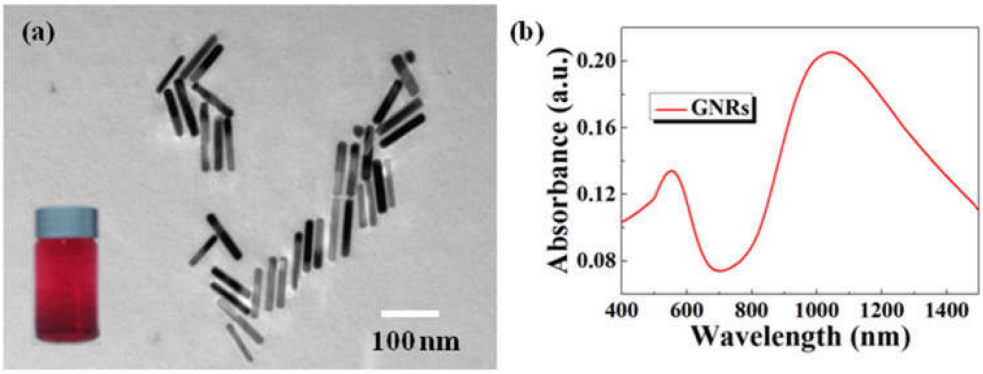

Fig. 1. (a) TEM image of GNRs (inset: Photograph of the aqueous solution of GNRs.); (b) The absorption spectrum of the GNRs.

solution. The color of the solution changed from yellow to dark brown immediately. This means the desired seed solution was obtained. The seed solution was kept at 60 °C for 1 hour and then used to synthesize GNRs. Next, we mixed 0.03 moles of CTAB, 0.0007 mol ortho-hydroxybenzoic, and 31.25 mL deionized water in a flask. After mixing, 0.156 mL of 0.00065 mol/L L-ascorbic acid aqueous solution, 1 mL of 0.004 mol/L $AgNO_3$ solution and 31.25 mL of 0.03375 mol/L $HAuCl_4$ aqueous solution was added into the growth solution and uniformly mixed. The color of the solution exhibits orange at once and then became colorless. 0.226 mL of 12 mol/L HCl solution was used to reduce the PH value below 7.0. Finally, we injected 0.2 mL of seed solution into the growth solution, so that it can initiate the growth of the GNRs. The final solution was kept at room temperature for 8 hours to ensure that it could successfully grow GNRs solution. Fig. 1(a) shows the transmission electron microscopy (TEM) image of the prepared GNRs. The rod-shape nanoparticles were obtained, and only a small amount of the spherical nanoparticles exists in the GNRs sample. The diameters of these GNRs were about 12 nm and the aspect ratios were in range of 4.5 to 8. There are almost 70% of GNRs have an aspect ratio of ∼5. The inset in Fig. 1(a) shows the photograph of the aqueous solution of GNRs. The GNRs film was formed by casting the GNRs-sodium carboxymetylcellulose (NaCMC) solution onto a flat silica glass, followed by a slow drying at room temperature.

The absorption spectrum of the GNRs film was shown in Fig. 1(b). We used the ultraviolet (UV)-visible-near infrared (NIR) spectrophotometer (UV-3600 Shimadzu) to measure the sample. It can be observed that the GNRs have two absorption peaks at 527 and 1080 nm, respectively. The absorption peak at 527 nm is caused by the transverse SPR of the GNRs or spherical nanoparticles, and the other absorption peak at 1080 nm results from the longitudinal SPR of GNRs. The broadband absorption from ∼800 nm to ∼1500 nm can be understood as the response from the GNRs with aspect ratios of from 4 to 8.

Subsequently, we used the open aperture Z-scan technique to measure the nonlinear absorption characteristics of the GNRs film [35]. The schematic diagram of the experimental system is shown in Fig. 2. The incident beam (repetition rate: 0.1 MHz, pulse width: 4 ns, center wavelength: 1064 nm) is split into two beams by a 1:1 beam splitter. One beam is received by probe 1 as the reference beam, and the other beam passes through a lens and vertically transmits the sample at the focal point, and then received by probe 2. During the experiment, the sample moves in the Z direction and the optical power values are recorded simultaneously.

The corresponding curve is shown in Fig. 3. The experimentally obtained data is fitted by the following formula:

$$T = 1 - \frac{\alpha_s}{1 + I/I_s} - \alpha_{\text{ns}}$$

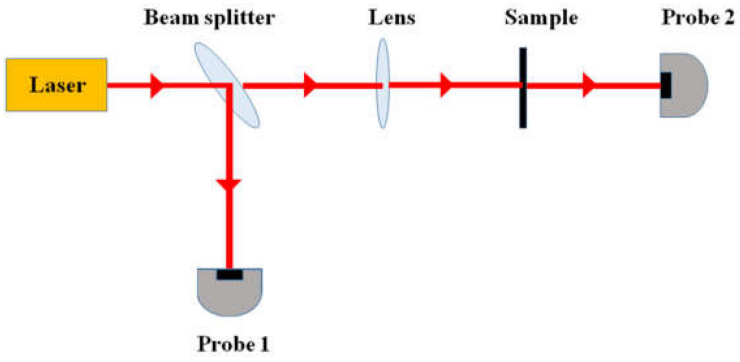

Fig. 2. Open aperture Z-scan experimental setup.

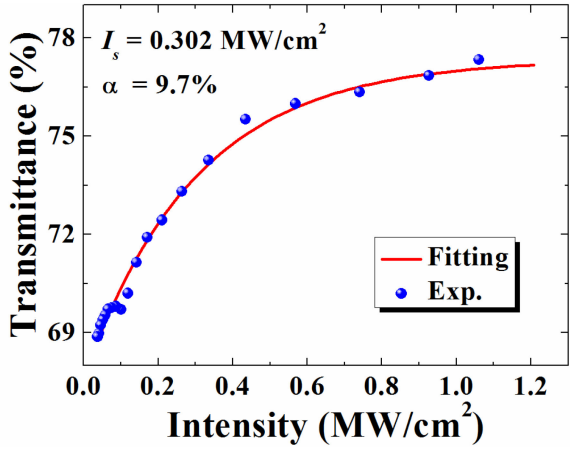

Fig. 3. The measured nonlinear absorption data of GNRs and its corresponding fitting curve at 1 μm.

where T is the optical transmittance, α_s is the normalized modulation depth, I is the peak intensity, I_s is the saturation intensity and α_{ns} is the non-saturable loss [36]. As the intensity increases, the transmittance also increases from ~69 to ~77%. By fitting the experimental data, we obtained the modulation depth of GNRs to be 9.7% and saturation intensity to be 0.302 MW/cm^2. The above results indicate that the non-linear absorption characteristics of GNRs SA could be used to modulate the Yb-doped fiber laser.

3. Results and Discussions

To examine whether GNRs SA can be used to induce mode locking, it was added to the YDFL cavity for verification. The schematic diagram is shown in Fig. 4. In the experiment, the total cavity length of the fiber laser is about 30 m, including 1 m high concentration ytterbium-doped fiber (LIEKKI Yb1200–4/125) with a group velocity dispersion of 24.22 ps^2/km and 20 m single mode light (SMF) with a group velocity dispersion of 21.91 ps^2/km. In addition to YDF, the pigtail of each device, including twisted fibers of PC, is a single mode fiber with a total length of about 9 m. A 980 nm laser diode is used as the pump source in the experimental setup. The pump light is looped through a wavelength division multiplexer (WDM), and then the 980 nm light is used to amplify the 1041 nm laser through the ytterbium-doped fiber as a gain medium. A 10:90 fiber coupler finally outputs 10% of the light. A polarization-independent isolator (PI-ISO) is used in the cavity to ensure unidirectional cycling of the laser and to isolate the returned light. In addition, the polarization controller (PC) was added to adjust the birefringence and the polarization of the

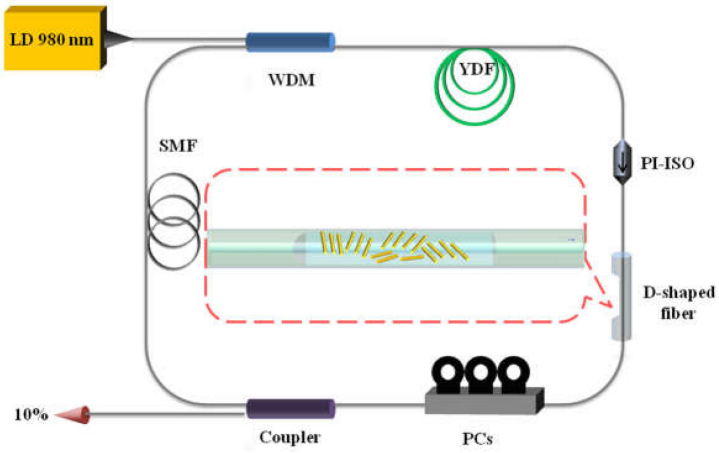

Fig. 4. The experimental setup of ytterbium-doped fiber laser passively mode locked using a GNRs SA.

cavity. When the D-shaped fiber with GNRs has not been added, the mode-locked pulse cannot be obtained by either increasing the power of the pump source or adjusting the PCs, which eliminate the possibility of self-mode locking. With the addition of the GNRs SA, the output modulation from continuous-wave light to mode-locked pulsed light can be achieved. Finally, to monitor mode-locked pulse characteristics and spectral properties, we connected the 10% output of the fiber coupler to a 500 MHz oscilloscope (Tektronix TDS3054B), an optical spectrum analyzer (Ando AQ-6317B), together with a 5 GHz photodetector (Thorlabs SIR5).

In the absence of the GNRs SA, the laser is always in the continuous-wave light state and is insensitive to changing the polarization state of the light. After introducing the GNRs SA, a stable mode-locked laser oscillation can be observed by adjusting the 980 nm pump power to 150 mW. Fig. 5(a) shows a typical oscilloscope pulse trains of a mode-locked laser operating pulse sequence at a pump power of 220 mW. The time interval between the two pulses is 150.5 ns, which corresponds to a repetition rate of 6.649 MHz. There is no significant intensity modulation, which indicates that the GNRs SA can well suppress the instability of the pulse output in the mode-locked laser. Besides, it can be seen from a digital oscilloscope that the pulse duration is about 160 ps. Fig. 5(b) shows a typical bell-shaped mode-locked output spectrum observed at 220 mW. The wavelength center is located at 1041 nm with a 3 dB bandwidth of $\sim$8.6 nm, which is measured by a spectral analyzer with a resolution of 0.015 nm. The time bandwidth product (TBP) of the laser pulse has been calculated to be 386.4, which indicates that the fiber laser is highly chirped. Inspired the requirements to obtain ultrafast laser output, the laser pulse can be compressed either externally or internally, and the nearly transform-limited output can be anticipated with optimized dispersion managements. Fig. 5(c) shows a single pulse profile with 220 mW pulse output. By fitting the measured points with a Gaussian function, the full width at half maximum (FWHM) of a single pulse is 162.3 ps. The radio frequency (RF) spectrum in Fig. 5(d) shows a clear peak at $\sim$6.65 MHz, which is consistent with the repetition rate of the mode-locked laser. The signal-to-noise ratio (SNR) of the RF spectrum is $\sim$77 dB. This result shows that the mode-locked pulse we obtained is highly stable.

When the pump power increases from 150 mW to 330 mW, the output power increases from 0.69 mW to 1.97 mW, corresponding to a slope efficiency of $\sim$0.7%. For the whole mode-locking operation, the nonlinear saturation absorption effect of the GNRs SA play an indispensable role for the dissipative soliton generation. As for the dispersion map of the Yb-doped fiber laser in the all normal dispersion regime, the spectral filtering effects, amplification, gain, and loss in the fiber resonator will contribute to the formation of soliton, i.e., dissipative soliton [37], [38]. Unlike traditional solitons, dissipative soliton can tolerate higher nonlinear effects and thus deliver the high energy pulse.

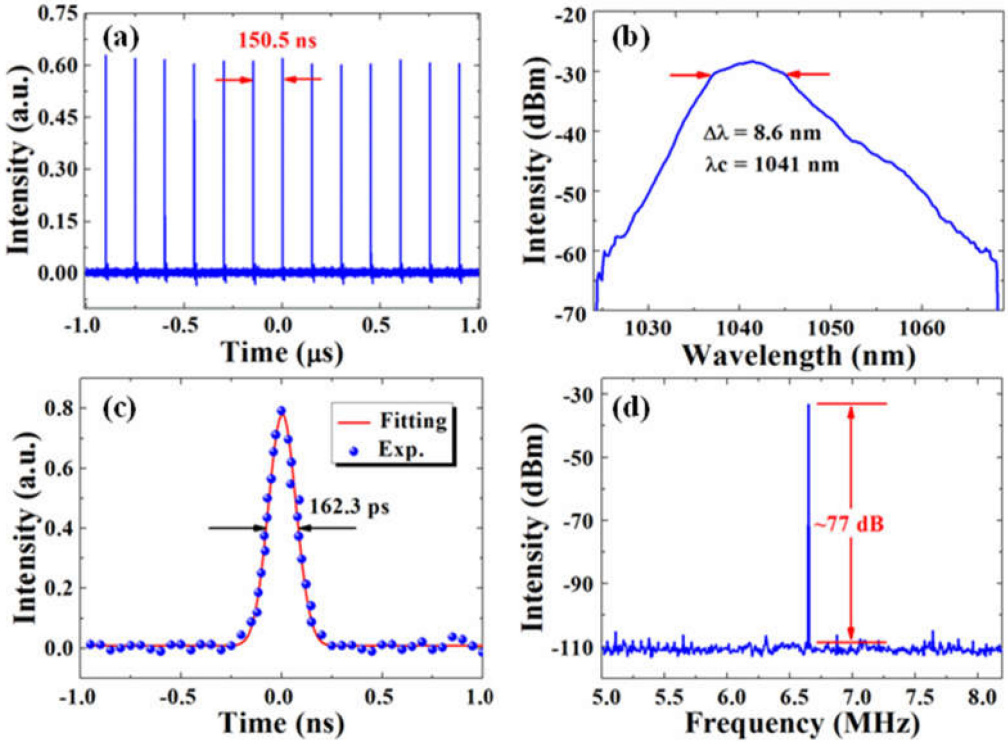

Fig. 5. (a) Typical oscilloscope pulse trains at a pump power of 220 mW; (b) the corresponding spectrum; (c) single pulse profile; (d) RF spectrum.

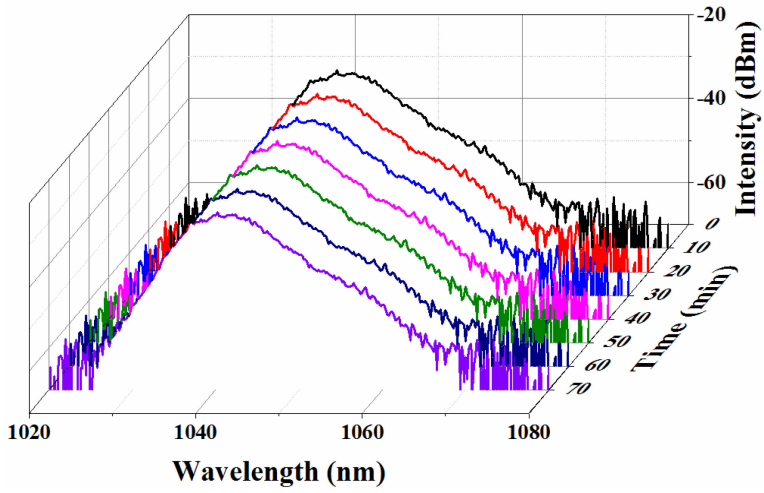

Fig. 6. Long term optical spectra measured under different time.

To study the long-term stability of single soliton pulse operation under the condition that the experimental conditions were not changed, the function of automatic recording of the spectrometer was used to record a set of pulse spectra every ten minutes as shown in Fig. 6. We can see that there is no drift in the center wavelength of the spectrum, the bandwidth of the spectrum is always consistent with the initial waveform, and no other frequency components appear, showing that the pulses we get are highly stable. During the transfer of gold nanorods to the D-shaped fiber, due to the high concentration of GNRs, sometimes the output power can't be well changed by controlling

TABLE 1
Laser Performance of the Mode-Locked Fiber Laser with GNR SA

Parameters / SA type	Wavelength (nm)	Energy (pJ)	Frequency (MHz)	Pulse duration (ps)	S/N (dB)	Ref.
FC/PC fiber connectors	1039	34.15	36.6	440	~50	[30]
	1039	33.79	43.5	460	/	[25]
	1560	56.18	35.6	2.91	/	[25]
Microfiber	1552	/	4.762	0.887	~53.8	[28]
D-shaped fiber	1068.2	/	18.69	460	~72	[31]
	1063.9	53	17.94	0.84	~73	[31]
	1041	197	6.649	162.3	~77	This work

"/": not available

the number of droplets of the GNRs. In the future work, we will try to obtain a mode-locked YDFL with higher output power and narrower pulse width by optimizing the SA and configurations of the laser cavity [39]–[41].

We have added a table to compare our experimental results with the reported results with GNRs SA, as show in Table 1. From the experimental results, it can be seen that the fiber laser modulated by GNRs exhibits better performance with regards to the pulse energy, S/N ratio and the all-fiberized laser setup.

4. Conclusions

In conclusion, we have achieved a stable all-fiberized passive YDFL via evanescent interaction with GNRs. We verified the nonlinear modulation of the GNRs experimentally. An absorption peak of GNRs is around 1100 nm, and its modulation depth is measured to be 9.7%. With the pump power above 150 mW, we can obtain a stable mode-locked output from the YDFL with repetition rate of ~6.65 MHz and SNR of ~77 dB. Our experimental results show that GNRs can be used as an efficient SA in YDFL, which can make inroads towards the nonlinear optics applications of plasmonic materials.

References

[1] M. J. F. Digonnet, *Rare-Earth-Doped Fiber Lasers and Amplifiers*. New York: Marcel Dekker, 1993.
[2] H. M. Pask, R. J. Carman, D. C. Hanna, and A. C. Tropper, "Ytterbium-doped silica fiber lasers: Versatile sources for the 1–1.2 μm region," *IEEE J. Sel. Top. Quantum Electron.*, vol. 1, no. 1, pp. 2–13, Apr. 1995.
[3] M. E. Fermann and I. Hartl, "Ultrafast fibre lasers," *Nature Photon.*, vol. 7, pp. 868–874, 2013.
[4] Q. Bao *et al.*, "Atomic-layer graphene as a saturable absorber for ultrafast pulsed lasers," *Adv. Func. Mater.*, vol. 19, pp. 3077–3083, 2009.
[5] Z. Sun *et al.*, "Graphene mode-locked ultrafast laser," *ACS Nano*, vol. 4, pp. 803–810, 2010.
[6] Y. Li *et al.*, "Graphene-assisted all-fiber optical-controllable laser," *IEEE J. Sel. Top. Quantum Electron.*, vol. 24, no. 3, May/Jun. 2018, Art. no. 0901709
[7] S. Yamashita *et al.*, "Saturable absorbers incorporating carbon nanotubes directlysynthesized onto substrates and fibersand their application to mode-locked fiber lasers," *Opt. Lett.*, vol. 29, pp. 1581–1584, 2004.
[8] F. Wang *et al.*, "Wideband-tuneable, nanotube mode-locked, fibre laser," *Nature Nanotechnol.*, vol. 3, pp. 738–742, 2008.
[9] K. N. Cheng, Y. H. Lin, S. Yamashita, and G. R. Lin, "Harmonic order-dependent pulsewidth shortening of a passively mode-locked fiber laser with a carbon nanotube saturable absorber," *IEEE Photon. J.*, vol. 4, no. 5, pp. 1542–1552, Oct. 2012.
[10] C. Zhao *et al.*, "Ultra-short pulse generation by a topological insulator based saturable absorber," *App. Phys. Lett.*, vol. 101, 2012, Art. no. 211106.
[11] C. Zhao *et al.*, "Wavelength-tunable picosecond soliton fiber laser with topological insulator: Bi_2Se_3 as a mode locker," *Opt. Exp.*, vol. 20, pp. 27888–27895, 2012.
[12] S. Chen, Q. Wang, C. Zhao, and Y. Li, "Stable single-longitudinal-mode fiber ring laser using topological iInsulator-based saturable absorber," *J. Lightw. Technol.*, vol. 32, no. 22, pp. 4438–4444, Nov. 2014.

[13] X. D. Wang *et al.*, "Nanocomposites with gold nanorod/silica core-shell structure as saturable absorber for femtosecond pulse generation in a fiber laser," *Opt. Exp.*, vol. 23, pp. 22602–22610, 2015.
[14] M. C. Daniel and D. Astruc, "Gold nanoparticles: Assembly, supramolecular chemistry, quantum-size-related properties, and applications toward biology, catalysis, and nanotechnology," *Chem. Rev.*, vol. 35, pp. 293–346, 2004.
[15] N. N. Lepeshkin, A. Schweinsberg, G. Piredda, R. S. Bennink, and R. W. Boyd, "Enhanced nonlinear optical response of one-dimensional metal-dielectric photonic crystals," *Phys. Rev. Lett.*, vol. 93, 2004, Art. no. 123902.
[16] W. A. Murray and W. L. Barnes, "Plasmonic materials," *Adv. Mater.*, vol. 19, pp. 3771–3782, 2007.
[17] A. Kumar, J. Prakash, D. S. Mehta, A. M. Biradar, and W. Haase, "Enhanced photoluminescence in gold nanoparticles doped ferroelectric liquid crystals," *Appl. Phys. Lett.*, vol. 95, 2009, Art. no. 023117.
[18] K. H. Kim, A. Husakou, and J. Herrmann, "Linear and nonlinear optical characteristics of composites containing metal nanoparticles with different sizes and shapes," *Opt. Exp.*, vol. 18, pp. 7488–7496, 2010.
[19] H. Chen, L. Shao, Q. Li, and J. Wang, "Gold nanorods and their plasmonic properties," *Chem. Soc. Rev.*, vol. 42, pp. 2679–2724, 2013.
[20] J. Koo, H. L. Ju, J. Lee, and W. Shin, "Large energy, all-fiberized Q-switched pulse laser using a GNRs/PVA saturable absorber," *Opt. Mater. Exp.*, vol. 5, pp. 1859–1867, 2015.
[21] I. Cohanoschi, A. Thibert, C. Toro, S. Zou, and F. E. Hernández, "Surface plasmon enhancement at a liquid–metal–liquid interface," *Plasmonics*, vol. 2, pp. 89–94, 2007.
[22] K. Tiwari, A. K. Singh, and S. C. Sharma, "Evidence for surface plasmons in a liquid crystal containing gold nanoparticles," *Appl. Phys. Lett.*, vol. 101, 2012, Art. no. 253103.
[23] D. Wu *et al.*, "Gold nanoparticles as a saturable absorber for visible 635 nm Q-switched pulse generation," *Opt. Exp.*, vol. 23, pp. 24071–24076, 2015.
[24] Z. Kang *et al.*, "Passively mode-locking induced by gold nanorods in erbium-doped fiber lasers," *Appl. Phys. Lett.*, vol. 103, 2013, Art. no. 041105.
[25] Z. Kang, X. Gao, L. Zhang, Y. Feng, G. Qin, and W. Qin, "Passively mode-locked fiber lasers at 1039 and 1560 nm based on a common gold nanorod saturable absorber," *Opt. Mater. Exp.*, vol. 5, pp. 794–801, 2015.
[26] T. Jiang, Y. Xu, Q. Tian, and L. Liu, "Passively Q-switching induced by gold nanocrystals," *Appl. Phys. Lett.*, vol. 101, 2012, Art. no. 151122.
[27] X. H. Li *et al.*, "All-normal-dispersion passively mode-locked Yb-doped fiber ring laser based on a graphene oxide saturable absorber," *Laser Phys. Lett.*, vol. 10, 2013, Art. no. 075108.
[28] X. D. Wang, Z. C. Luo, H. Liu, M. Liu, A. P. Luo, and W. C. Xu, "Microfiber-based gold nanorods as saturable absorber for femtosecond pulse generation in a fiber laser," *Appl. Phys. Lett.*, vol. 105, 2014, Art. no. 161107.
[29] X. D. Wang *et al.*, "Gold nanorod as saturable absorber for Q-switched Yb-doped fiber laser," *Opt. Commun.*, vol. 346, pp. 21–25, 2015.
[30] Z. Kang *et al.*, "Gold nanorod saturable absorber for passive mode-locking at 1 μm wavelength," *Laser Phys. Lett.*, vol. 11, no. 3, 2014, Art. no. 035102.
[31] J. Lee, J. Koo, and J. H. Lee, "Femtosecond mode-locking of an ytterbium-doped fiber laser using self-assembled gold nanorods," *Laser Phys. Lett.*, vol. 14, no. 9, p. 090001, 2017.
[32] B. Nikoobakht and M. A. Elsayed, "Preparation and growth mechanism of gold nanorods (NRs) using seed-mediated growth method," *Chemistry Mater.*, vol. 15, pp. 1957–1962, 2003.
[33] X. Ye *et al.*, "Improved size-tunable synthesis of monodisperse gold nanorods through the use of aromatic additives," *ACS Nano*, vol. 6, pp. 2804–2817, 2012.
[34] X. Ye, Y. Gao, J. Chen, D. C. Reifsnyder, C. Zheng, and C. B. Murray, "Seeded growth of monodisperse gold nanorods using bromide-free surfactant mixtures," *Nano Lett.*, vol. 13, pp. 2163–2171, 2013.
[35] G. Jiang *et al.*, "Tunable gold nanorods Q-switcher for pulsed Er-doped fiber laser," *IEEE Photon. J.*, vol. 9, no. 5, Oct. 2017, Art. no. 6102009.
[36] H. I. Elim, J. Yang, J. Y. Lee, J. Mi, and W. Ji, "Observation of saturable and reverse-saturable absorption at longitudinal surface plasmon resonance in gold nanorods," *Appl. Phys. Lett.*, vol. 88, 2006, Art. no. 083107.
[37] Y. D. Cui, X. M. Liu, and C. Zeng, "Conventional and dissipative solitons in a CFBG-based fiber laser mode-locked with a graphene-nanotube mixture," *Laser Phys. Lett.*, vol. 11, no. 5, 2014, Art. no. 055106.
[38] C. Chi, J. Lee, J. Koo, and J. H. Lee, "All-normal-dispersion dissipative-soliton fiber laser at 1.06 μm using a bulk-structured Bi_2Te_3 topological insulator-deposited side-polished fiber," *Laser Phys.*, vol. 24, no. 10, 2014, Art. no. 105106
[39] S. S. Huang *et al.*, "High order harmonic mode-locking in an all-normal-dispersion Yb-doped fiber laser with a graphene oxide saturable absorber," *Laser Phys.*, vol. 24, 2013, Art. no. 015001.
[40] B. Xu, A. Martinez, S. Y. Set, C. S. Goh, and S. Yamashita, "A net normal dispersion all-fiber laser using a hybrid mode-locking mechanism," *Laser Phys. Lett.*, vol. 11, 2014, Art. no. 025101.
[41] D. Fan, C. Mou, X. Bai, S. Wang, N. Chen, and X. Zeng, "Passively Q-switched erbium-doped fiber laser using evanescent field interaction with gold-nanosphere based saturable absorber," *Opt. Exp.*, vol. 22, pp. 18537–18542, 2014.